Tahr density estimates from aerial surveys - preliminary results

Dave Ramsey - Arthur Rylah Institute, 123 Brown Street Heidelberg, Victoria 3084.

9/7/2018

RELEASED UNDER THE OFFICIAL INFORMATION ACT

1 Summary

Aerial surveys of Himalayan tahr were undertaken on 38, 2 x 2 km plots sampled across the tahr range during 2016 and 2017. Density and abundance estimates from each plot were then used to estimate total tahr abundance on public conservation land as well as for each tahr management unit. The total abundance of tahr on public conservation land was estimated to be 35,633, with a 95% confidence interval of 17,347 - 53,920 tahr. Average tahr density within management units ranged from 10.3/km^2 to 0.23/km^2. Tahr density in the two exclusion zones averaged 0.06/km^2 for MU E2 and 0.34/km^2 for MU E1. Average tahr density was higher than the management threshold of 2.5 tahr/km^2 on all management units except MU 7.

Analysis of ungulate faecal pellet monitoring data conducted at each plot indicated inconsistent relationships between tahr density and the faecal pellet index (FPI). Additional data collection undertaken during 2018 may shed futher light on these relationships.

2 Introduction

The Himalayan Tahr Control Plan (Department of Conservation 1993) defines intervention densities in terms of number of tahr per km^2 in each of seven management units (range: <1 to 2.5 tahr per km^2) and two exclusion zones (0 per km^2). Currently, it is intended that information on tahr abundance be collected from tier 1 plots located in the tahr management zone using faecal pellet sampling (Forsyth 2016). One obvious issue that arises is how to link the data on faecal pellet abundance to actual tahr abundance so that these can be linked to the control plan intervention densities. Hence, it is proposed that a calibration exercise be undertaken to estimate the relationship between tahr faecal pellet index and tahr densities (Forsyth 2016). Calibration is to be undertaken by estimating tahr density on 30 randomly selected tier 1 plots from the tahr management zone using aerial surveys from a helicopter. Abundance was to be estimated by monitoring a 2 x 2 km plot overlaid on the location of tier 1 plots where the faecal pellets monitoring is undertaken. Helicopter monitoring involved three seperate counts of tahr seen within each 2 x 2 km plot. Each count was undertaken at least 14 days apart to minimise the disturbance effects of the helicopter on each replicate count.

In order to undertake a robust assessment of the relationship between tahr abundance (estimated from repeat helicopter counts) and faecal pellet counts (estimated from the 4 transects at each tier 1 sampling location), a number of issues have to be resolved. The first issue is that faecal pellets counts could consist of pellets of several ungulate species such as deer, chamois and tahr as these cannot be distinguished from pellet morphology. However, it is proposed that DNA sampling of fresh pellets be undertaken to estimate species composition of nominal "ungulate" pellets. The second issue is that the repeat aerial counts at each 2 x 2 km plot are undertaken at least 14 days apart. While this was necesary to reduce disturbance of tahr by the helicopter (which could bias estimates), it raises an additional issue in that it may not be reasonable to consider the plot "closed" during the entire sampling period (i.e approximately 1-2 months between the 1st and 3rd count). Here lack of "closure" means that tahr abundance could change during the sampling period due to either immigration to, or emigration from, the plot.

During 2016, 16 2 x 2 km plots were sampled with a further 22 sampled in 2017 giving a total of 38 plots available for analysis. Here I analyse the aerial survey data obtained from the 38 sampled plots to estimate tahr abundance assuming the tahr population on each plot was open to movement related changes

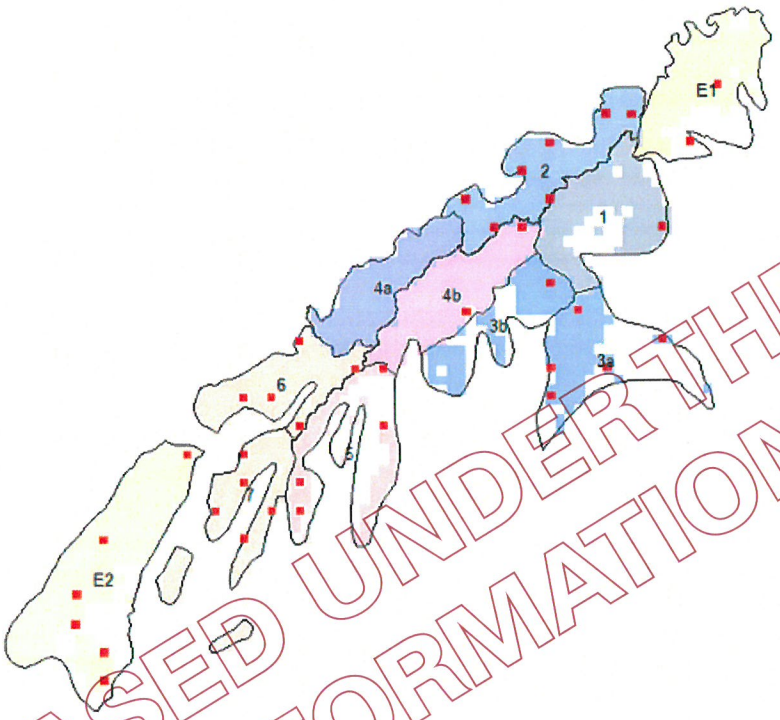

Figure 1: Location of the 38 sampled 2 x 2 km plots where helicopter counts of tahr were undertaken. Red squares indicate plot locations. Colour shaded area indicates the DOC PCL and black polyons indicate the tahr management zones.

between replicate surveys. I then examine the relationship between thar density and the ungulate pellet presence/absence data from the 38 plots to examine whether a relationship between the two looks feasible.

3 Methods

Helicopter count survey was available from 38, 2 x 2 km plots sampled over the period 1/2/2016 to the 29/4/2017 (Figure 1). Although each plot was nominally 4 km^2 in area, this only indicated the 2D surface area of the plot. Due to the steep terrain on most plots, the actual surface area covered by each 2 x 2 km area could vary considerably from the nominal 4 km^2. Hence, to calculate the actual 3D surface area of each plot, each 2 x 2 km area was divided into 400 1-ha cells and the surface area of each cell calculated using a 15m digital Elevation Model (DEM). The 3D surface areas of each 1-ha cell were then added to give the 3D surface area for each plot. The 3D surface area was subsequently used for all density calculations for each plot.

3.1 Abundance estimation

The counts of tahr at each plot, at each sampling occasion, were used to estimate abundance corrected for imperfect detection using an N-mixture model for open populations (Dail & Madsen 2011). Hence, this

RELEASED UNDER THE OFFICIAL INFORMATION ACT

model was able to account for movement of tahr on or off the plot between the three sampling occassion. Further details of this model are provided in Appendix 1.

In order to compare tahr density with pellet counts obtained from the tier 1 plots, we estimated an average abundance for each plot as the mean of the estimates from the three sampling occasions. Tahr density was estimated by dividing the abundance estimate by the 3D area of each plot. The mean tahr density for each management unit was then calculated as the mean density across the plots that occurred in each unit.

To estimate the total abundance of tahr within each management unit, we assumed that the sampled plots consisted of a stratified random sample of the total available plots that could have been sampled within each management unit, with management units forming the strata. We assumed a two-stage sampling design where the overall estimate of abundance within each unit was composed of two sources of error, the spatial variation in tahr density among plots within each unit and the estimation error associated with the abundance estimate for each plot. Total abundance within each management unit was then estimated as the mean plot abundance in the unit multiplied by the total available plots within each unit. The total number of available plots within each unit was calcuated by subdividing the (2D) area of conservation land within the unit into 2 x 2 km plots. Variance of the estimates of total tahr abundance within each stratum and overall abundance was calculated using finite sampling methods (Skalski 1994). More details on these calculations are provided in Appendix 2.

3.2 Pellet counts

Ungulate pellet monitoring was conducted at each plot using two methods. The first method used the ungulate pellet monitoring data collected at each tier 1 monitoring location. This involved a count of total pellets and pellet groups from four transects (30 plots per transect) radiating from the corners of the permenant 20m vegetation monitoring plot. The second method involved measuring the presence or absence of ungulate pellet along 8 transects (5 plots per transect) radiating out from center, sides and corners of the 20 m vegetation plot.

Estimates of the faecal pellet index of ungulates (FPI) at each site were expressed as either the number of pellets or pellet groups per plot (method 1) or the proportion of plots containing ungulate pellets (pellet prevalence) (method 2). The estimated FPI was plotted against tahr density estimated from the 2 x 2 km survey region covering each tier 1 plot to assess the relationship between FPI and tahr density. Assuming a reasonable relationship exists, it would then be desirable to calibrate FPI so it could be expressed as an estimate of thar density. In addition to thar density estimates from the 2 x 2 km survey region (i.e. 4 km^2), we also examined relationships between FPI and tahr density, over subsets of the total survey region (i.e. 1 km^2, 2 km^2 and 3 km^2) to detemine whether a smaller survey region could be used to estimate thar density from helicopter counts.

RELEASED UNDER THE OFFICIAL INFORMATION ACT

4 Results

4.1 Tahr density and abundance

The mean density of tahr on each plot varied widely, from zero to 28 thar/km^2 (Figure 2). However, precision of some of the mean density estimates was low due to the high variation in thar density over the three sampling occasions at some plots (Figure 3). The corresponding mean density of tahr within each management unit was also highly variable (Table 1). Average tahr density was higher than the management threshold of 2.5 tahr/km^2 on all management units except MU 7. Tahr density in the two exclusion zones averaged 0.06/km^2 for MU E2 and 0.34/km^2 for MU E1. No sampling was undertaken on management unit 4a (Table 1).

Table 1: Mean Density of tahr (thar/km2) within each management unit. SD - standard deviation; lcl - lower 95% confidence interval; ucl - upper 95% confidence interval

MU	Density	SD	lcl	ucl	n
1	6.19	2.34	3.22	11.98	2
2	5.37	7.14	0.00	22.99	6
3	7.88	7.64	0.00	25.63	6
4	3.58	3.93	0.00	11.53	2
5	10.25	12.30	0.14	39.41	4
6	3.10	2.33	0.65	9.09	5
7	0.23	0.42	0.00	1.37	5
E1	0.34	0.38	0.00	1.25	2
E2	0.06	0.14	0.00	0.42	6

The total abundance of tahr across all sampled management units was estimated to be 35,638, with a 95% confidence interval of 17,347 - 53,920. Estimates of total tahr abundance were made for management units with at least two sampled plots (i.e. exluding MU 3b). Total abundance ranged from around 8000 tahr estimated to occur in MU 3, to a total of 102 tahr estimated to occur in exclusion zone E2 (Table 2). In general, the precison of the abundance estimates for individual management units was fairly poor with estimates having wide confidence intervals (e.g. the 95% confidence interval for MU 4 was 967 - 46,516 tahr!). This was a consequence of small sample sizes for most management units (relative to the total number of plots available for sampling) as well as the high spatial variation in abundance estimates among plots within a unit. Despite this, the precison of the estimate of total abundance was acceptable, having a coefficient of variation of 25%.

Table 2: Estimates of total abundance of tahr within each sampled management unit (N). SD - standard deviation; lcl - lower 95% confidence interval; ucl - upper 95% confidence interval;u - number of sampled plots; U - estimated number of plots available to be sampled

unitID	Nhat	SD	lcl	ucl	u	U
1	6166	1795	3485	10910	2	195
2	5757	3215	1927	17199	6	206
3	8168	3232	3761	17737	6	219
4	6705	6626	967	46516	2	372
5	5696	3606	1647	19697	4	112
6	2541	671	1515	4264	5	167
7	174	122	44	684	5	151
E1	324	288	57	1850	2	191
E2	102	42	46	227	6	343

RELEASED UNDER THE OFFICIAL INFORMATION ACT

4.2 Relationships between tahr density and FPI

Pellet counts were undertaken for 36 of the 38 tahr tier 1 plots. The estimates of ungulate FPI as indexed by ungulate pellet prevalence, pellets/plot or pellet groups/plot revealed inconsistent relationships with tahr density on the 4 km^2 survey region (Figure 4). Scatterplots of FPI against thar densities on smaller subregions of the survey area (1 km^2, 2 km^2 or 3 km^2) revealed similar inconsistent relationships with tahr

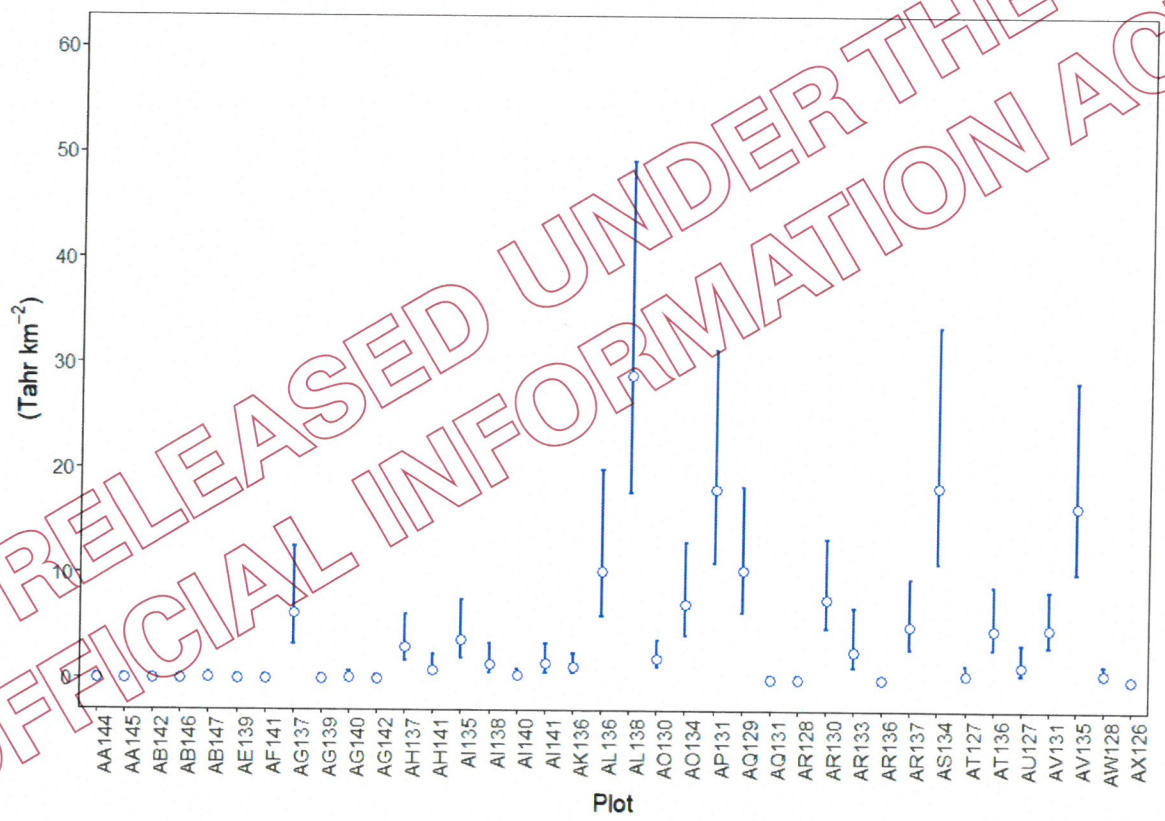

RELEASED UNDER THE OFFICIAL INFORMATION ACT

Figure 2: The estimates of average density of tahr on each sampled plot.

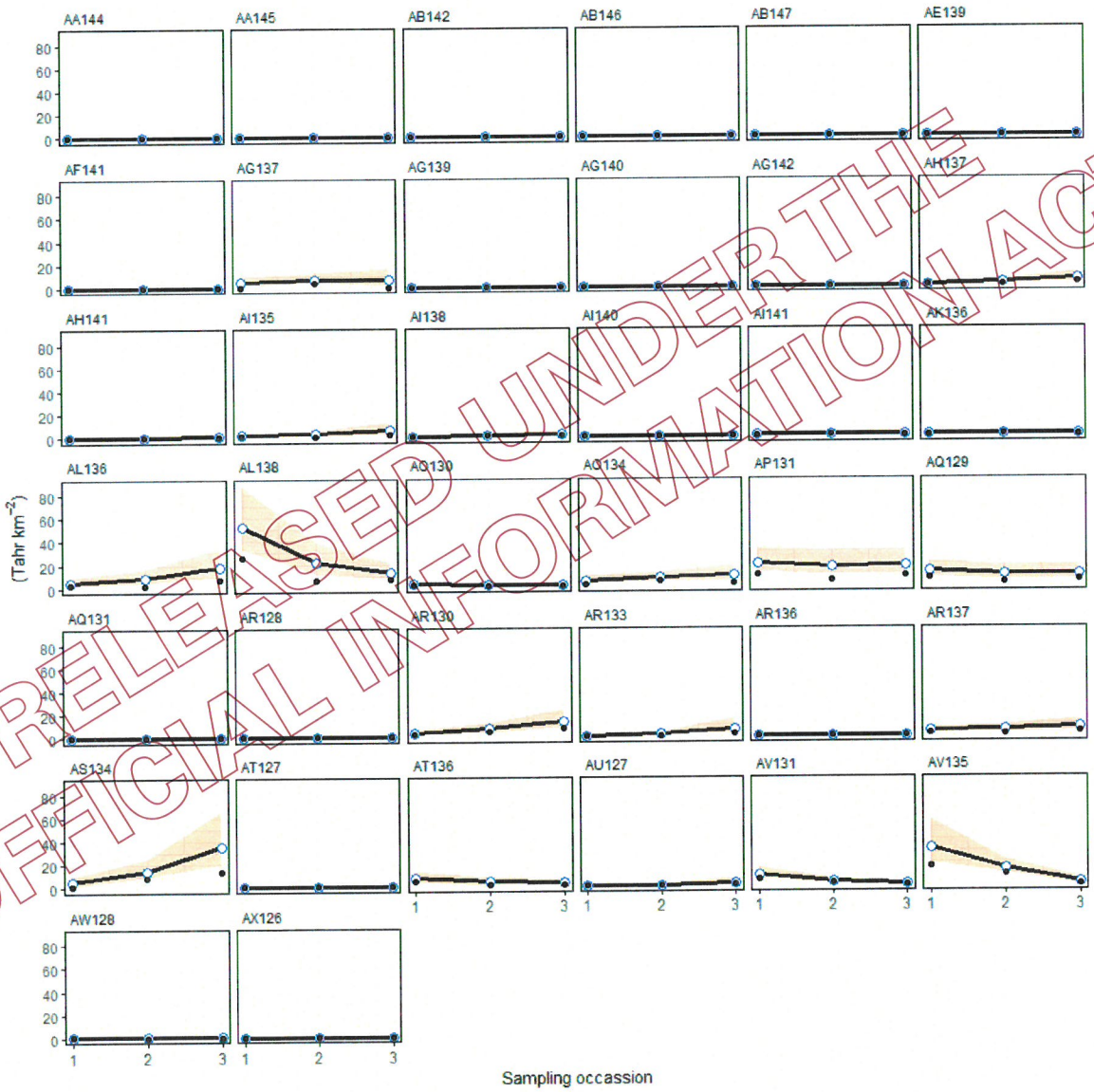

Figure 3: The estimates of thar density for each sampling occassion for each of the 38 sampled plots (blue open circles and lines). Black solid circles are the naive density calculated from the raw counts.

RELEASED UNDER THE OFFICIAL INFORMATION ACT

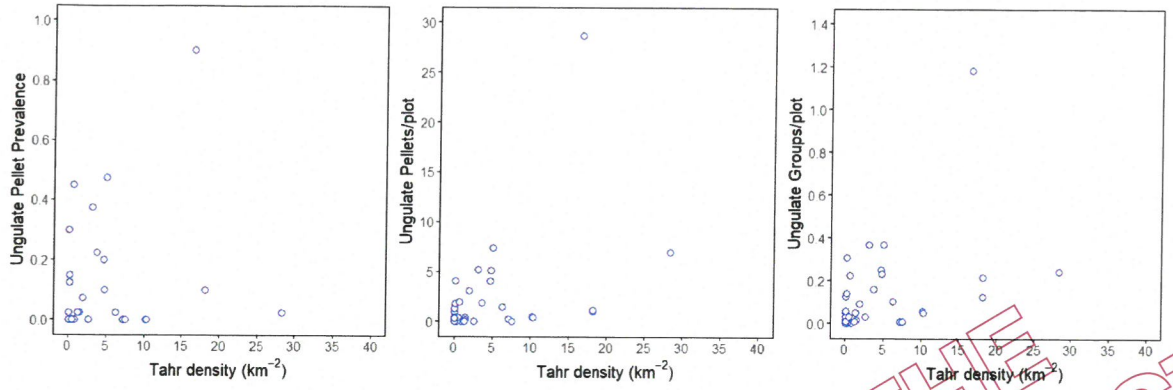

Figure 4: Scatterplot of the relationship between ungulate pellet prevalence (left), total pellets/plot (middle) and pellet groups/plot (right) and estimated average tahr density on the 4 km2 survey region at 36 of the 38 sampled plots.

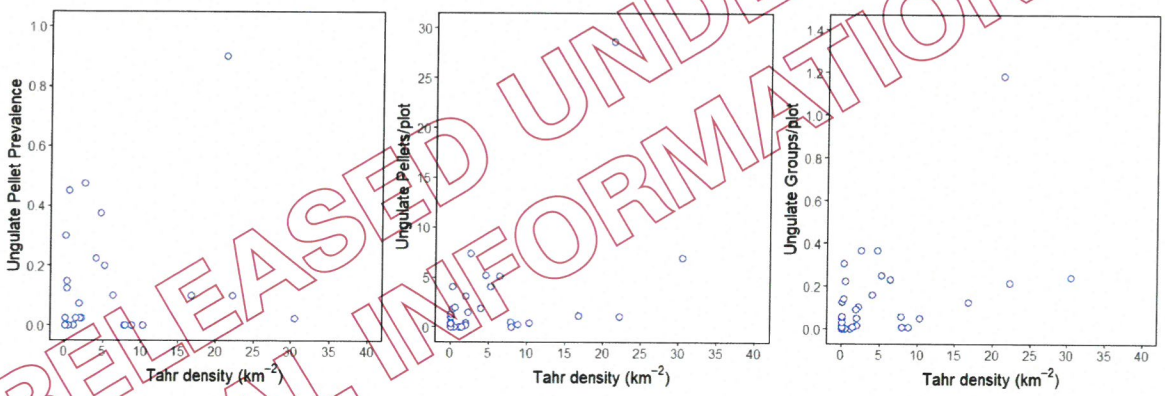

Figure 5: Scatterplot of the relationship between ungulate pellet prevalence (left), total pellets/plot (middle) and pellet groups/plot (right) and estimated average tahr density on the 3 km2 survey region at 36 of the 38 sampled plots.

RELEASED UNDER THE OFFICIAL INFORMATION ACT

density (Figure 5-7). Given the uncertain nature of these relationships. formal calibration of FPI with tahr density was not attempted.

5 Discussion

Tahr densities were highly variable across the tahr management zones with average densities exceeding the threshold of 2.5/km^2 from the tahr managememnt plan for all zones except MU 7, E1 and E2. Average tahr densities were also greater than zero in the exclusion zones. However, the estimates for the exclusion zones also included zero in their 95% credible interval despite a single tahr being seen in sampled plots in zone E2 and 4 tahr seen in zone E1. The reason the credible intervals include zero for these zones is that the density estimate is the mean of the estimates over the three sampling occasions and, as the model allows movement of tahr between sampling occasions, the estimate for any one occasion could be zero.

Precision of total tahr abundance estimates for each management zone were generally poor, due mainly to the small numbers of sampled plots within each MU. Total abundance estimates were also highly dependent on the estimate of the number of plots within each zone that could have been sampled. This was estimated

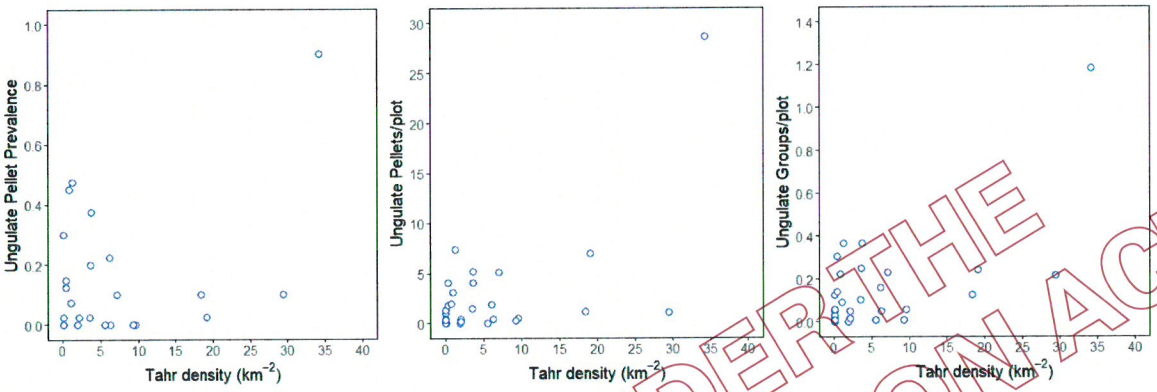

Figure 6: Scatterplot of the relationship between ungulate pellet prevalence (left), total pellets/plot (middle) and pellet groups/plot (right) and estimated average tahr density on the 2 km2 survey region at 36 of the 38 sampled plots.

RELEASED UNDER THE OFFICIAL INFORMATION ACT

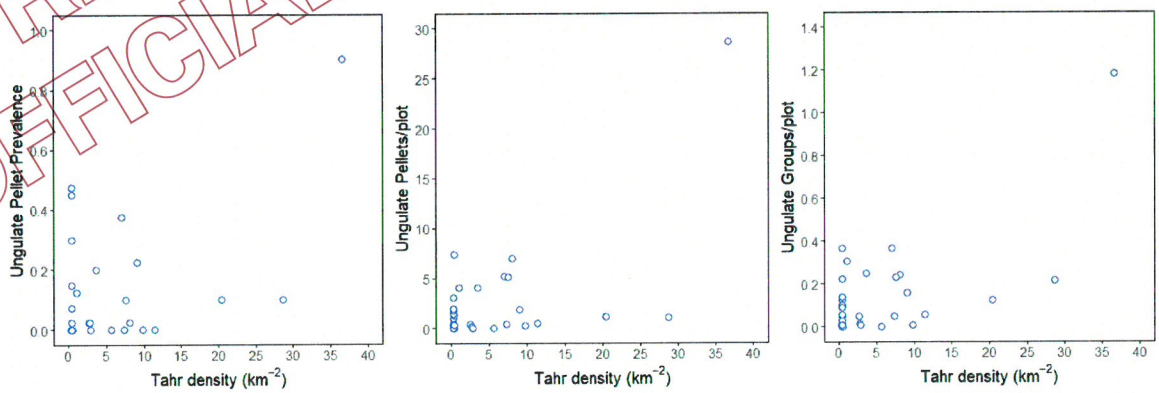

Figure 7: Scatterplot of the relationship between ungulate pellet prevalence (left), total pellets/plot (middle) and pellet groups/plot (right) and estimated average tahr density on the 1 km2 survey region at 36 of the 38 sampled plots.

using a map of the DOC PCL overlaid on the MU boundaries. However, it is highly likely that not all of this area may be suitable for tahr, which would induce bias in estimates of total abundance. Hence, more detailed maps of available tahr habitat would improve estimates. Alternatively, a model of the relationship between tahr abundance and habitat type would provide a means to more accurately map the distribution of tahr across the management area. However, inital attempts at identifying relationships between tahr abundance and habitat type have not been successful.

The relationship between tahr abundance and ungulate FPI from both the presence/absence plots and the pellet counts conducted during regular tier one sampling did not reveal signs of a predictable relationship. This uncertainty was present at all spatial scales examined (i.e. tahr density estimated on search areas of 1 - 4 km^2). This uncertainty was mainly due to some sites having a high FPI at low tahr density. The presence of other ungulates could be one cause of the high FPI on sites with low tahr abundance and future work should include an investigation into relationships between total ungulate density from aerial surveys and FPI. Another cause could be the fact that pellets have likely accumulated over several months, while tahr densities were estimated over approximately one month, and were themselves, subject to some uncertainty. Hence, due to the uncertain nature of the relationship between FPI and thar abundance, no formal calibration of FPI with tahr density was undertaken. Additional data collection scheduled for 2017/18 may shed further light on these relationships.

6 References

Dail, D. & Madsen, L. (2011). Models for Estimating Abundance from Repeated Counts of an Open Metapopulation. *Biometrics*, **67**, 577–587.

Forsyth, D. (2016). *Tier 1 Himalayan tahr abundance monitoring protocol.* Arthur Rhylah Institute, Heidelberg, VIC.

Plummer, M. (2003). JAGS: A Program for Analysis of Bayesian Graphical Models Using Gibbs Sampling. pp. 1–10. Proceedings of the 3rd International Workshop on Distributed Statistical Computing (DSC 2003), Vienna, Austria.

Skalski, J.R. (1994). Estimating Wildlife Populations Based on Incomplete Area Surveys. *Wildlife Society Bulletin*, **22**, 192–203.

Thompson, S.K. (1992). *Sampling.* John Wiley & Sons, New York.

Thompson, W.L., White, G.C. & Gowan, C. (1998). *Monitoring Vertebrate Populations*, 1st edn. Academic Press. Retrieved from http://www.amazon.com/dp/0126889600

RELEASED UNDER THE OFFICIAL INFORMATION ACT

7 Appendix 1

7.1 Abundance model

The counts of thar at each plot, at each time period, were used to estimate abundance corrected for imperfect detection using an N-mixture model for open populations (Dail & Madsen 2011). We treated each of the three replicate counts at each plot as potentially being open to movement (immigration/emigration) between sampling times. Hence, thar abundance at each site i and sampling period t ($t = 1..3$) was modeled as

$$y_{it} \sim Bin(p_i, N_{i,t})$$

In order to estimate abundance $N_{i,t}$ at each sampling period t, it is assumed that abundance follows a first order Markov process where abundance at time t is dependent on the abundance at time t-1, as well as movement parameters $(N_{i,t}|N_{i,t-1}, \omega, \gamma)$. This was achieved by decomposing $N_{i,t}$ as the sum of two random variables

$$S_{i,t}|N_{i,t} \sim Bin(N_{i,t-1}, \omega_i)$$
$$G_{i,t}|N_{i,t} \sim Poisson(\gamma_i(N_{i,t-1}))$$

where $S_{i,t}$ and $G_{i,t}$ are the additions and losses to the population at a plot at time t with γ_i and ω_i representing movement parameters (immigration and emmigration, respectively) for each plot (Dail & Madsen 2011). In order to compare thar density with pellet counts obtained from the Tier 1 plots, we estimated an average density for each plot as the mean of the estimates from the three surveys. Thar density was estimated by dividing the abundance estimate by the area of the survey region (4 km^2).

The N-mixture open population model above was fitted in a Bayesian framework using Markov Chain Monte Carlo (MCMC) sampling using `JAGS ver.3.3.0` (Plummer 2003). The movement and detection probability parameters (ω_i, γ_i) were modeled as hierarchical random effects on either the log (γ) or logit (ω) scale as $N(\mu, \tau)$. Weakly informative priors were placed on the hyperparameters ($\mu \sim N(0, 10)$) and $\tau \sim \text{half} - t(4)$. The model was updated for 120,000 iterations using 3 chains with the first 20,000 iterations used as a burn-in and discarded. To reduce autocorrelation, each chain was thinned by keeping every 10th sample leaving a total of 10,000 samples from each chain with which to form the posterior distribution of the parameters.

RELEASED UNDER THE OFFICIAL INFORMATION ACT

8 Appendix 2

8.1 Abundance estimates for each management unit

We used finite sampling estimators assuming a stratified random sampling design ((Skalski 1994, Thompson *et al.* (1998), Thompson (1992))) to estimate total abundance witin each stratum, based on incomplete surveys. Here, management units correspond to strata. If u number of plots are sampled from a total number U in stratum h, the estimate of abundance is given by

$$\hat{N}_h = \overline{N_h} U_h$$

where $\hat{N}_h$ is the estimate of total abundance for stratum h, $\overline{N_h}$ is the mean abundance over the u plots and U_h is total number of plots in stratum h. The estimate of variance is given by

$$\hat{Var}(\hat{N}_h) = U_h^2 \left\{ (1 - \frac{u_h}{U_h}) \frac{\hat{S}^2_{N_{hi}}}{u_h} + \frac{\overline{\hat{Var}(\hat{N}_{hi}|N_{hi})}}{U_h} \right\}$$

where

$$\hat{S}^2_{N_{hi}} = \frac{\sum_{k=1}^{u} (\hat{N}_{hi} - \overline{\hat{N}_h})^2}{u_h - 1}$$

and

$$\overline{\hat{Var}(\hat{N}_{hi}|N_{hi})} = \frac{\sum_{k=1}^{u_h} \hat{Var}(\hat{N}_{hi}|N_{hi})}{u_h}$$

The total abundance over all sampled management units is then simply

$$\sum_{h=1}^{n} \hat{N}_h$$

with variance

$$\sum_{h=1}^{n} \hat{Var}(\hat{N}_h)$$

RELEASED UNDER THE OFFICIAL INFORMATION ACT

RELEASED UNDER THE
OFFICIAL INFORMATION ACT